



# HHS Public Access

Author manuscript

*Bioconjug Chem.* Author manuscript; available in PMC 2018 June 17.

Published in final edited form as:

*Bioconjug Chem.* 2018 February 21; 29(2): 538–545. doi:10.1021/acs.bioconjchem.8b00028.

## Bioorthogonal Masking of Circulating Antibody–TCO Groups Using Tetrazine-Functionalized Dextran Polymers

Jan-Philip Meyer<sup>†,iD</sup>, Kathryn M. Tully<sup>†,‡</sup>, James Jackson<sup>†</sup>, Thomas R. Dilling<sup>†</sup>, Thomas Reiner<sup>\*,†,§</sup>, and Jason S. Lewis<sup>\*,†,‡,§,||</sup>

<sup>†</sup>Department of Radiology, Memorial Sloan Kettering Cancer Center, 1275 York Avenue, New York, New York 10065, United States

<sup>||</sup>Program in Molecular Pharmacology, Memorial Sloan Kettering Cancer Center, 1275 York Avenue, New York, New York 10065, United States

<sup>‡</sup>Department of Pharmacology, Weill Cornell Medical College, 1300 York Avenue, New York, New York 10065, United States

<sup>§</sup>Department of Radiology, Weill Cornell Medical College, 1300 York Avenue, New York, New York 10065, United States

### Abstract

Pretargeting strategies have gained popularity for the *in vivo* imaging and therapy of cancer by combining antibodies with small molecule radioligands. *In vivo* recombination of both moieties can be achieved using the bioorthogonal inverse electron demand Diels–Alder (IEDDA) chemistry between tetrazine (Tz) and *trans*-cyclooctene (TCO). An issue that arises with pretargeting strategies is that while part of the antibody dose accumulates at antigen-expressing tumor tissue, there is a significant portion of the injected antibody that remains in circulation, causing a reduction in target-to-background ratios. Herein, we report the development of a novel TCO scavenger, the masking agent DP–Tz. DP–Tz is based on Tz-modified dextran polymers (DP, MW = 0.5–2 MDa). Large dextran polymers were reported to exhibit low penetration of tumor vasculature and appeared nontoxic, nonimmunogenic, and easily modifiable. Our newly developed masking agent deactivates the remaining TCO-moieties on the circulating mAbs yet does not impact the tumor uptake of the Tz-radioligand. In pretargeting studies utilizing a <sup>68</sup>Ga-labeled tetrazine radioligand ([<sup>68</sup>Ga]Ga-NOTA-PEG<sub>11</sub>-tetrazine), DP–Tz constructs (Tz/DP ratios of 62–254) significantly increased TTB ratios from 0.8 ± 0.3 (control cohorts) to up to 5.8 ± 2.3 at 2 h postinjection. Tumor tissue delineation in PET imaging experiments employing DP–Tz is

\*Corresponding Authors. lewisj2@mskcc.org. Phone: +1 (646) 888-3038 (J.S.L). reinert@mskcc.org. Phone: +1 (646) 888-3461 (T.R.).

ORCID 

Jan-Philip Meyer: 0000-0003-4252-370X

### ASSOCIATED CONTENT

Supporting Information

The Supporting Information is available free of charge on the ACS Publications website at DOI: 10.1021/acs.bioconjchem.8b00028.

General experimental and equipment information, chemical structures and additional data of all precursor molecules, representative radio-HPLC traces, *ex vivo* biodistribution data and additional PET imaging data (PDF)

The authors declare no competing financial interest.

significantly increased compared to control. Uptake values of other significant organs, such as heart, lungs, pancreas, and stomach, were decreased on average by 2-fold when using DP–Tz. Overall, pretargeting experiments utilizing DP–Tz showed significantly improved tumor delineation, enhanced PET image quality, and reduced uptake in vital organs. We believe that this new masking agent is a powerful new addition to the IEDDA-based pretargeting tool box and, due to its properties, an excellent candidate for clinical translation.

## Graphical abstract



## INTRODUCTION

Dextrans are nontoxic, nonimmunogenic, and water-soluble glucose polymers that are commercially available. Chemically, dextran polymers (DPs) are complex branched glycans with variable chain lengths. Glucose molecules are interconnected via  $\alpha$ -1,3- and  $\alpha$ -1,6-glycosidic bonds, making these polymers not only stable under mild acidic and basic conditions but also biologically inert while circulating in the blood plasma.<sup>1,2</sup> Consequently, DPs have found wide application in medicine from blood volume expanders to drug delivery systems, with Dextran 70 being on the WHO list of essential medicines.<sup>2–4</sup> The use of DPs as drug delivery agents is based on their ability to increase the plasma half-lives (PHL) and bioavailabilities of therapeutic agents that would otherwise clear from circulation too fast to elicit strong pharmacokinetic effects.<sup>5</sup> Another important size-dependent property of DPs is tissue penetration. As the molecular size of the molecule increases, vascular permeability decreases.<sup>6</sup> This is important for drug delivery systems that aim for deep tissue penetration in order to deposit an effective amount of drug.

Another possibility to obtain improved drug delivery to target tissue is pretargeting. Particularly important for this study, pretargeting has gained popularity for the *in vivo* imaging and therapy of cancer. Pretargeting approaches strive to retain the exquisite specificity and affinity of monoclonal antibodies (mAbs) for *in vivo* discrimination between antigen-positive and antigen-negative tissues while evading the limitations associated with the slow pharmacokinetics of antibodies. After administration and appropriate circulation time of the antibody, a small-molecule hapten carrying the radioactive payload with fast-clearing pharmacokinetics (PK) can be administered.<sup>7–10</sup> *In vivo* recombination of both moieties can be achieved using a bioorthogonal ligation reaction, if both the mAb as well as the small molecule carry complementary functionalities that allow effective *in vivo* reactivity. The use of bioorthogonal click chemistry in pretargeting, particularly the inverse electron demand Diels–Alder (IEDDA) reaction between tetrazine (Tz) and *trans*-cyclooctene (TCO), has shown promising preclinical results.<sup>8–12</sup> By utilizing IEDDA chemistry, a TCO-modified mAb is injected and allowed to reach the target site within a mAb-specific accumulation time interval, before a Tz-containing small molecule that clears rapidly from circulation is administered.

Several groups, including ours, have previously demonstrated the feasibility of the IEDDA-based pretargeting approach for the *in vivo* imaging and therapy of disease, using Tz radioligands labeled with both diagnostic (e.g.,  $^{68}\text{Ga}$ ,  $^{18}\text{F}$ ,  $^{64}\text{Cu}$ ,  $^{111}\text{In}$ ) and therapeutic (e.g.,  $^{177}\text{Lu}$ ) radionuclides.<sup>7–11,13–15</sup> Recently, we investigated a library of  $^{68}\text{Ga}$ - and  $^{18}\text{F}$ -labeled Tz radioligands for their performance in pretargeted positron emission tomography (PET) imaging experiments. The identified lead compounds enabled clear tumor delineation as early as 2 h post injection with excellent dosimetric properties.<sup>16</sup> For a review of the Tz/TCO IEDDA reaction in medical imaging, please see Altai et al. 2017.<sup>17</sup>

However, an issue that arises with pretargeting strategies is that while part of the antibody dose accumulates at antigen-expressing tumor tissue, there is a significant portion of the injected antibody that remains in circulation. When the small molecule radiotracer is injected, it reacts with the antibodies both in circulation and at the tumor site, causing a reduction in target-to-background ratios.

Various efforts have been made to develop clearing agents (CA) that bind circulating antibody and accelerate their clearance from circulation.<sup>18–22</sup> With importance for the study presented herein, the use of dextran-based clearing agents has previously been reported in pretargeting applications using a DOTA-containing hapten and anti-DOTA-bispecific mAbs.<sup>18,19,21,22</sup> Using a fusion protein with affinity for CD20 and DOTA, Orcutt et al. demonstrated in pretargeted radioimmunotherapy (PRIT) experiments improved target-to-background ratios when a nonradioactive dextran-DOTA-Yttrium construct was injected prior to the radioligand.<sup>21</sup> The dextran construct was injected 1 day after the administration of the fusion protein and 1 h before the injection of the  $^{90}\text{Y}$ -labeled biotin small molecule effector probe.

Shortly thereafter, Rossin et al. reported the development of clearing agents for IEDDA-based pretargeting, involving  $^{177}\text{Lu}$ -labeled Tz radioligands and the anti-TAG71 mAb CC49-TCO.<sup>20</sup> Two Tz-functionalized, macromolecular clearing agents were evaluated for their ability to increase target-to-background ratios in PRIT experiments: galactose-albumin-tetrazine and polystyrene beads coated with tetrazine-conjugated albumin. Significantly increased tumor-to-background ratios as well as elevated absolute tumor uptake values were reported, demonstrating their potential in pretargeting.

Herein, we present the synthesis and *in vivo* evaluation of a novel, inexpensive, and easy-to-synthesize tetrazine-functionalized dextran polymer (DP-Tz) for the bioorthogonal masking of circulating TCO-mAb in IEDDA-based pretargeting strategies. We investigated the *in vivo* performance of DP-Tz via noninvasive pretargeted PET imaging and *ex vivo* biodistribution at 2 h post radiotracer injection (unless stated otherwise) using one of our recently developed  $^{68}\text{Ga}$ -labeled tetrazine constructs, [ $^{68}\text{Ga}$ ]Ga-NOTA-PEG<sup>11</sup>-tetrazine (Scheme 1, herein referred to as [ $^{68}\text{Ga}$ ]1).<sup>16</sup> We utilized the established CA19.9-expressing pancreatic ductal adenocarcinoma (PDAC) cell line BxPC3 with the anti-CA19.9 mAb 5B1, as this model was used in previous work to evaluate the pharmacokinetic properties of the [ $^{68}\text{Ga}$ ]1 tracer, and the A33-expressing colorectal cancer (CRC) model SW1222 in combination with A33-targeting mAb huA3.<sup>9,16</sup> Our results demonstrate that the newly developed DP-Tz conjugates effectively deactivate circulating mAb-TCO, resulting in

increased target-to-background ratios with significantly elevated tumor-to-blood (TTB) ratios and without impairing tumoral tracer uptake (Figure 1).

## RESULTS

### Synthesis and *in Vivo* Evaluation of Modified Dextran Polymers

Reaction conditions for the conjugation of Tz–NHS to DP–NH<sub>2</sub> were varied in order to determine optimal conditions to achieve both the highest overall yields and Tz/DP ratios (Scheme 2, Table S1). DP–Tz constructs with the highest isolated yields and the highest Tz/DP ratios of  $\approx 600$  (run # 9,10) were obtained using 2,000 kDa DP–NH<sub>2</sub> (38.1 mg, 19.1 nmol, dissolved in 900  $\mu$ L of PBS) and Tz–NHS (18 mg, 57.5  $\mu$ g, dissolved in 50  $\mu$ L of DMF) incubated for 2 h at 37 °C with agitation (700 rpm) at pH 8.5. Purity of DP–Tz constructs was determined to >95% using size-exclusion HPLC before and after the conjugation reaction of Tz–NHS to DP–NH<sub>2</sub> (Figures S1 and S2). Reactivity of conjugated Tz moieties was confirmed by incubating DP–Tz with 5B1–TCO (2-fold excess) in PBS (250  $\mu$ L) at room temperature for 15 min. The mixture was analyzed using size-exclusion HPLC, confirming click reaction between DP–Tz and 5B1–TCO by the absence of the 525 nm absorption of the Tz moiety (Figure S3).

In order to first track the biodistribution of the DP–Tz, the DP–Tz construct obtained from run #4 (Table S1) was used for further functionalization with the <sup>89</sup>Zr-chelator DFO. Zirconium-89 was selected so that the biodistribution of the DP–Tz constructs could be evaluated up to 144 h post injection. For pretargeting experiments, we used the short-lived [<sup>68</sup>Ga]1. Upon purification DP–Tz–DFO conjugates were incubated with <sup>89</sup>Zr at pH = 6.8. A maximum conversion of  $\approx 30\%$  was achieved, and prolonging the incubation time to up to 24 h did not increase conversion (Section 2.2, Supporting Information). BxPC3-tumor bearing mice were preinjected with 5B1–TCO 2 h prior to injection with <sup>89</sup>Zr–DP–Tz–DFO. This time frame was chosen so that the 5B1–TCO did not have enough time to accumulate at the tumor site and would therefore be representative of circulating mAb for pretargeting applications. Biodistribution of <sup>89</sup>Zr–DP–Tz–DFO was then monitored via PET imaging (2–144 h post injection, Figure S6).

Imaging data showed that the majority of radioactivity accumulated in the liver as early as 2 h post injection, ( $41.7 \pm 5.4\%$ ID/g) with only background activity concentrations in the blood pool, kidneys, spleen, and lung. Biodistribution did not significantly change over the course of this experiment (up to 48 h post injection), with the liver as the only organ with significant uptake at 48 h post injection ( $33.2 \pm 3.1\%$ ID/g). These results suggest that our modified DP is rapidly cleared from the blood pool via the hepatobiliary pathway as quickly as 2 h post injection, without having significant tumor accumulation by itself. This would likely be different if a smaller dextran was used, as these have shown to have higher vascular permeability and can therefore serve as pretargeted radiotracers themselves.<sup>23</sup>

After tracking the biodistribution of modified DPs, we sought to determine the effect of DP–Tz on the biodistribution of the mAb (here 5B1–TCO) over time. For that, we modified 5B1 with both TCO and DFO groups that allowed us to radiolabel 5B1 with <sup>89</sup>Zr while retaining the ability to undergo click reaction. Labeling the 5B1–TCO with zirconium-89 (instead of

gallium-68) enabled us to track the biodistribution of 5B1 over time, with and without DP-Tz present. We expected DP-Tz to undergo click chemistry with  $^{89}\text{Zr}$ -5B1-TCO-DFO in circulation to form mAb-DP conjugates, which would prevent 5B1 from reaching the target site resulting in reduced tumor uptake. Two cohorts ( $n = 5$ ) of BxPC3-tumor bearing mice were injected with  $^{89}\text{Zr}$ -5B1-TCO-DFO (1.3 nmol/mouse). The experimental group received DP-Tz (Run #10, Tz/DP = 600, 200 nmol Tz/mouse) 20 min after the injection of  $^{89}\text{Zr}$ -5B1-TCO-DFO. The 20 min latency period between  $^{89}\text{Zr}$ -5B1-TCO-DFO and DP-Tz injections was chosen in order to ensure that the majority of the  $^{89}\text{Zr}$ -5B1-TCO-DFO would still remain in circulation upon injection with DP-Tz, and we could evaluate the effect of DP-Tz on the biodistribution of the mAb. PET Imaging of both cohorts was conducted 1 and 24 h post injection of  $^{89}\text{Zr}$ -5B1-TCO-DFO (Figure 2). This study yielded the anticipated results: the cohort that received DP-Tz showed a significant ( $\approx 5$ -fold) reduction in tumoral uptake compared to the control group of  $5.8 \pm 2.3\% \text{ID/g}$  as compared to  $26.2 \pm 7.9\% \text{ID/g}$ , respectively. Thus, DP-Tz effectively reacts with circulating mAb-TCO in the bloodstream and should be as effective in pretargeting experiments.

### Pretargeting Experiments Using DP-Tz as a Masking Agent for Circulating mAb-TCO

After evaluating the biodistribution of DP-Tz constructs alone and in combination with 5B1-TCO, we subsequently investigated the impact of DP-Tz in pretargeting experiments. A first proof-of-concept *in vivo* study was conducted in athymic nude mice with s.c. BxPC3 tumor model. 5B1-TCO was injected 72 h prior to DP-Tz (Figure 3a). Tz-DP (run #10, Table S1) was administered 0.5 and 0.25 h prior to [ $^{68}\text{Ga}$ ]1 using 2 different concentrations corresponding to 120 and 24 nmol Tz per mouse, respectively (Figure 3a). The two lag times of 0.5 and 0.25 h between DP-Tz and [ $^{68}\text{Ga}$ ]1 were chosen to determine the impact of lag time on masking efficacy. Indeed, all cohorts that received Tz-DP showed significantly increased TTB and TTO ratios. TTB ratios ranged from  $5.8 \pm 2.3$  for group 1 compared to  $0.7 \pm 0.2$  for the control group (Figure 3b-d). Differences in TTB ratios between the experimental groups were not statistically significant. Full biodistribution data (Figure 3b) showed reduced radioactivity concentrations in vital organs such as heart, liver, intestines, and kidney. PET imaging experiments further demonstrated improved TTB ratios and clear tumor delineation for essentially all groups that were treated with DP-Tz (Figure 3d).

Subsequently, we investigated whether the results can be reproduced in athymic nude mice with s.c. colorectal cancer tumors using the SW1222 cell line. HuA33-TCO was injected 48 h prior to DP-Tz (Figure 4a). Tz-DP (run #1, Table S1) with a Tz/DP ratio of  $\approx 52$  was injected at 2 different time points (2 and 0.5 h) and in 2 different concentrations (0.68 and 32 nmol of Tz-DP, corresponding to 34 and 16 nmol Tz per mouse, respectively) prior to [ $^{68}\text{Ga}$ ]1. All 3 cohorts that received Tz-DP showed significantly increased TTB ratios of up to  $3.2 \pm 0.5$  compared to  $0.8 \pm 0.2$  of the control group (Figure 4b). Again, there was no significant difference between cohorts when changing the lag time between injection of DP-Tz and [ $^{68}\text{Ga}$ ]1. PET imaging studies confirmed those results by showing significantly decreased blood pool radioactivity concentrations with excellent tumor delineation at 2 h post injection compared to the control mice (Figure 4c).

## DISCUSSION

Over the past few years, pretargeting has become increasingly important in the noninvasive imaging of disease as well as in radioimmunotherapy applications.<sup>7–11,13–16,18–22,24</sup> Despite recent advancements, it has been recognized that the use of scavenging agents to remove residual circulating mAb from the blood pool prior to the injection of the small molecule effector probe may lead to improved target-to-background contrast.<sup>18–22</sup> With regard to IEDDA-based bioorthogonal click chemistry, Rossin et al. successfully introduced polystyrene-based particles coated with Tz moieties for the removal of residual circulating mAb–TCO.<sup>20</sup>

Herein, we present the synthesis and *in vivo* evaluation of a novel and easy-to-synthesize dextran-based TCO masking agent — DP–Tz — that effectively deactivates circulating mAb–TCO in IEDDA-based pretargeting studies. The main advantages of this TCO masking agent are its easy, inexpensive, and scalable synthesis as well as its low toxicity and immunogenicity. Reaction conditions for Tz-functionalization of the DPs were optimized and finally yielded consistently high and reproducible results. Using the 2,000 kDa DP–NH<sub>2</sub> (2,800 reactive amines/polymer) we achieved high Tz conjugation yields of  $\approx 600$  Tz moieties/DP in high purities (>95%).

<sup>89</sup>Zr-labeled DP–Tz alone showed accumulation and retention in the liver after 2 h post injection in PET imaging experiments. Notably, though, clearance of DP–Tz/antibody conjugates is not necessary for the success of our agent. DP–Tz is a true scavenging and masking agent, eliminating the ability of antibodies to bind to tetrazines, making them invisible for any injected radiotracer. The observed pharmacokinetic profile of our DP–Tz is in line with previously published data that showed that dextran polymers exhibited rapid blood clearance and hepatic uptake when injected in low concentrations of 1 mg/kg.<sup>5,25</sup> Subsequently, we examined the effect of DP–Tz on the biodistribution of an antibody by using <sup>89</sup>Zr-labeled 5B1–DFO–TCO constructs. For that, BxPC3-tumor bearing mice were injected with <sup>89</sup>Zr-labeled 5B1–DFO–TCO, with the experimental cohort receiving DP–Tz 20 min later. Our study showed that tumor uptake of <sup>89</sup>Zr-labeled 5B1 in mice that received DP–Tz was 5-fold lower compared to the control group, demonstrating that DP–Tz effectively and irreversibly binds 5B1–DFO–TCO through click chemistry. Bioorthogonal IEDDA chemistry attached the mAb to the DP thereby preventing 5B1 from reaching the tumor site. It was assumed that the tumor uptake observed in the DP–Tz treated mice was due to the 20 min lag time that was applied between 5B1–TCO and DP–Tz injections. A small fraction of the mAb thus possessed the time to reach the target site prior to DP–Tz injection. DP–5B1 click adducts that formed in circulation showed increased uptake in organs of the lymphatic system, such as spleen and lymph nodes, simply due to their size.

In order to test whether this newly developed masking agent is capable of increasing tumor-to-background ratios in pretargeting experiments, we carried out a pilot study in BxPC3-tumor bearing mice that were preinjected with 5B1–TCO. After 72 h, DP–Tz was injected using different concentrations and different time points, followed by the administration of [<sup>68</sup>Ga]1. All experimental groups that received DP–Tz showed at least a 3-fold increase in TTB ratios 2 h post injection when compared to the control group with regular pretargeting

conditions. No statistical difference in TTB ratios was found between the experimental groups, suggesting that the reduced amount of DP-conjugated Tz (24 nmol) is sufficient for quantitative masking of the antibody. Additionally, reducing the time window between DP-Tz and [ $^{68}\text{Ga}$ ]I injections from 30 to 10 min did not affect the efficacy of DP-Tz. This implies that clinically, a diagnostic radioisotope could be injected after just 10 min after administration of DP-Tz, which could happen via the same port, only slightly increasing the wait time between tracer injections and PET scan.

We subsequently conducted an additional pretargeting study using the SW1222-tumor bearing mice that were preinjected with huA33-TCO. The aim of this study was to reproduce the results obtained with the BxPC3 model and to validate this technique in terms of robustness when used in different pretargeting systems. We used a time window of 2 h and 30 min between DP-Tz and [ $^{68}\text{Ga}$ ]I injections and again administered DP-Tz in two different concentrations. The results of this study confirmed our previous findings, with significantly higher TTB ratios of the treated cohorts compared to the control groups that did not receive DP-Tz. Varying the concentrations or shortening the time window between DP-Tz and [ $^{68}\text{Ga}$ ]I showed no significant differences in TTB ratios. These data suggest that 16 nmol of Tz per injection is sufficient to achieve high TTB ratios and that higher Tz/DP ratios are not necessarily required for improved pretargeting performance. Further experiments focusing on the dose-dependency in pretargeting studies will be critical to determine the minimum amount of DP-Tz required to achieve improved diagnostic performance.

Overall, this study reports the development of a masking agent that significantly improved TTB ratios and overall image contrast in  $^{68}\text{Ga}$ -based pretargeting experiments. Importantly, our dextran-based masking agent DP-Tz can be rapidly synthesized due to inexpensive and straightforward bioconjugation chemistry. We believe that DP-Tz adds significant value to existing pretargeting strategies for diagnostic applications. Further, the clinically validated nontoxic and nonimmunogenic nature of these dextran polymers makes this approach suitable for applications in clinical pretargeted cancer diagnostics.

## CONCLUSION

In sum, a novel masking agent, DP-Tz for IEDDA-based pretargeting applications, was developed and validated *in vivo*. Pretargeting experiments utilizing DP-Tz showed significantly improved PET image quality and TTB ratios, as well as reduced off-target organ uptake compared to the regular IEDDA-based pretargeting approach. This nontoxic, inexpensive, and easy-to-synthesize agent has particularly high potential in pretargeting applications that utilize short-lived radionuclides such as  $^{68}\text{Ga}$  and  $^{18}\text{F}$  where images and biodistribution data have to be acquired at early time points (4 h post injection). We believe this new agent to be of value in future diagnostic and therapeutic IEDDA-based pretargeting strategies. Due to its nontoxic and nonimmunogenic character, this masking agent may be a promising candidate to support the clinical translation of IEDDA-based pretargeting.

## MATERIALS AND METHODS

### Dextran–Tetrazine Conjugation

DP–Tz constructs were synthesized by incubating amino-dextran (DP–NH<sub>2</sub>, MW = 0.5 and 2 MDa, 1–36.9 mg, 2–18.5 nmol) with an excess (>10<sup>3</sup> eq) of Tz–NHS ester (2–8 mg, 6.5–25 μmol), resulting in Tz/DP ratios of 62–654, depending on utilized dextran and reaction conditions (Scheme 2, Section 2.1 Supporting Information, Table S1). DP–NH<sub>2</sub> was dissolved in PBS (800 μL, pH = 7.4) before the pH was adjusted to 8.5–9 using 0.1 M Na<sub>2</sub>CO<sub>3</sub> (≈40 μL). Tz–NHS ester was dissolved in DMF (20–40 μL) and slowly added to the aqueous solution containing DP–NH<sub>2</sub>. The mixture was incubated at room temperature with agitation (700 rpm) for 2 h. Subsequently, DP–Tz conjugates were purified using PD-10 size-exclusion columns using metal-free water and were subsequently lyophilized. The purity of Tz–DP was determined using size–exclusion HPLC (0.9% saline, 0.75 mL/min). The dried construct was weighed and dissolved in PBS, and Tz/DP ratios were then calculated using UV/vis spectroscopy. Constructs were dissolved and stored in PBS at –80 °C.

### Dextran–Tz–DFO Conjugation and <sup>89</sup>Zr-Labeling

DP–Tz–DFO constructs were synthesized by incubating amino-dextran (2,000 kDa, 5 mg, 2.5 nmol) first with an excess of Tz–NHS ester (2–8 mg, 6.5–25 μmol), resulting in Tz/DP ratios of 110 ± 22 (*n* = 3) after purification as described above (Section 3.1, Supporting Information). The DP–Tz constructs were subsequently incubated with a 25-fold molar excess of DFO–NCS ester at pH = 8.5 in carbonate buffer. DP–Tz–DFO conjugates were finally purified using PD-10 desalting columns. DP–Tz–DFO constructs were then labeled with <sup>89</sup>Zr using an aqueous buffer (pH = 6.8) at 37 °C for 1 h with 500 rpm agitation. Conversion and radiochemical purity was determined via iTLC (mobile phase: 50 mM EDTA, pH = 5). Labeling yields of approximately 30% were achieved (Figure S4), and longer incubation times (> 24 h) did not lead to higher radiolabeling yields. The radiolabeled product fraction was purified using PD-10 desalting columns.

### Radiosynthesis of [<sup>68</sup>Ga]1

<sup>68</sup>Ga-Labeled Tz-radioligand [<sup>68</sup>Ga]1 for pretargeting experiments was synthesized as previously described.<sup>16</sup> Briefly, precursor 1 (48 μg, 31 nmol) was incubated with <sup>68</sup>Ga<sup>3+</sup> in acetate buffer (pH = 4.5) for 10 min at 40 °C and 700 rpm (Scheme 1). [<sup>68</sup>Ga]1 was purified using a preconditioned C18 cartridge, eluted in 200 μL of EtOH, and diluted with 0.9% saline to achieve <10% v/v EtOH for subsequent injections. [<sup>68</sup>Ga]1 was obtained in high isolated radiochemical yields (RCY, >80%) and purities (>97%) with molar activities of >11 MBq/nmol.

### Antibody–TCO Conjugation

Antibody-modification (5B1 and huA33, 3–4 mg) using TCO–NHS ester was conducted as previously described.<sup>8,9,16</sup> Briefly, purified mAb (3–4 mg) was dissolved in PBS/carbonate buffer (pH = 8.5) and subsequently incubated with TCO–NHS ester (30–35 equiv) at 37 °C for 90 min. The immunoconjugate was then purified using PD-10 desalting columns. The



number of TCO-groups per mAb was determined according to a previously described procedure using an AF488-Tz construct.

### Antibody-DFO-TCO Conjugation and $^{89}\text{Zr}$ -Labeling

TCO-conjugation of 5B1 was performed as described above, except that 25 equiv of TCO-NHS was used instead of 30–35 equiv as for the regular TCO-modification. Purified 5B1-TCO (2–3 mg) was subsequently incubated with a 20-fold molar excess of DFO-NCS at pH = 8.5 in carbonate buffer. The resulting 5B1-DFO-TCO conjugates were purified using PD-10 desalting columns, and the number of TCO-groups per mAb was determined as described above. 5B1-DFO-TCO constructs were radiolabeled with  $^{89}\text{Zr}$  using an aqueous buffer (pH = 6.8) at 37 °C for 1 h with 500 rpm agitation. Conversion and radiochemical purity was determined via iTLC (mobile phase: 50 mM EDTA, pH = 5). Quantitative labeling yields were achieved using this labeling protocol, despite the modification with two different functionalities (Supporting Information, Section 3.2.).

### Biodistribution of $^{89}\text{Zr}$ -Labeled DP-Tz-DFO Constructs

$^{89}\text{Zr}$ -Labeled DP-Tz-DFO conjugates (0.2 nmol) were administered into BxPC3-tumor bearing mice ( $n = 3$ ) 2 h after the injection of 5B1-TCO (1.2 nmol) via the lateral tail vein. Control animals ( $n = 3$ ) did not receive 5B1-TCO. PET imaging was performed 2, 24, 48, and 144 h post injection of  $^{89}\text{Zr}$ -DP-Tz-DFO (Supplementary Section 2.3).

### Investigation of *in Vivo* Click Chemistry between DP-Tz and 5B1-DFO-TCO

We labeled 5B1-DFO-TCO with  $^{89}\text{Zr}$  and determined how the biodistribution of the mAb is influenced upon injection of DP-Tz. For that, BxPC3-tumor bearing mice were injected with  $^{89}\text{Zr}$ -5B1-DFO-TCO. After 20 min, mice of the experimental cohort received DP-Tz (Tz = 200 nmol/mouse), whereas the control group did not receive DP-Tz. PET imaging of both cohorts was performed 1 and 24 h post injection of  $^{89}\text{Zr}$ -5B1-DFO-TCO. *Ex vivo* biodistribution data were obtained for the last time point (24 h) for both cohorts ( $n = 5$ ).

### Pretargeting Studies Determining *in Vivo* Performance of DP-Tz Constructs

The *in vivo* performance of the newly developed DP-Tz constructs was measured by comparing TTB and tumor-to-organ (TTO) ratios as well as absolute tumoral tracer uptake in experiments using Tz-DP compared to standard pretargeting experiments. PET imaging studies and *ex vivo* organ biodistribution experiments were performed 2 h post [ $^{68}\text{Ga}$ ]1 injection. For pretargeting studies ( $n = 4$ ) huA33-TCO (150  $\mu\text{g}$ , 0.7 nmol/mouse) and 5B1-TCO (180  $\mu\text{g}$ , 1.2 nmol/mouse) were injected 48 and 72 h prior to [ $^{68}\text{Ga}$ ]1 (1.2–1.8 equiv relative to mAb), respectively. Tz-DP constructs (0.15–0.3 nmol = 16–200 nmol Tz per mouse) dissolved in PBS were injected 120–10 min prior to [ $^{68}\text{Ga}$ ]1. Injected amounts and time points of DP-Tz administration were varied in order to determine optimal conditions.

### Statistical Analysis

Data were analyzed by the unpaired, two-tailed Student's *t* test. Differences at the 95% confidence level ( $P < 0.05$ ) were considered to be statistically significant.

## Supplementary Material

Refer to Web version on PubMed Central for supplementary material.

## Acknowledgments

The authors gratefully acknowledge the MSKCC Small Animal Imaging Core Facility as well as the Radiochemistry and Molecular Imaging Probe core, which were supported in part by NIH grant P30 CA08748. The authors also would like to thank the NIH (F32 CA210396, J.P.M.). We also thank Wolfgang W. Scholz and MabVax Therapeutics (San Diego, CA) for providing the fully human monoclonal antibody 5B1. We gratefully acknowledge Mr. William H. and Mrs. Alice Goodwin and the Commonwealth Foundation for Cancer Research and The Center for Experimental Therapeutics of Memorial Sloan Kettering Cancer Center.

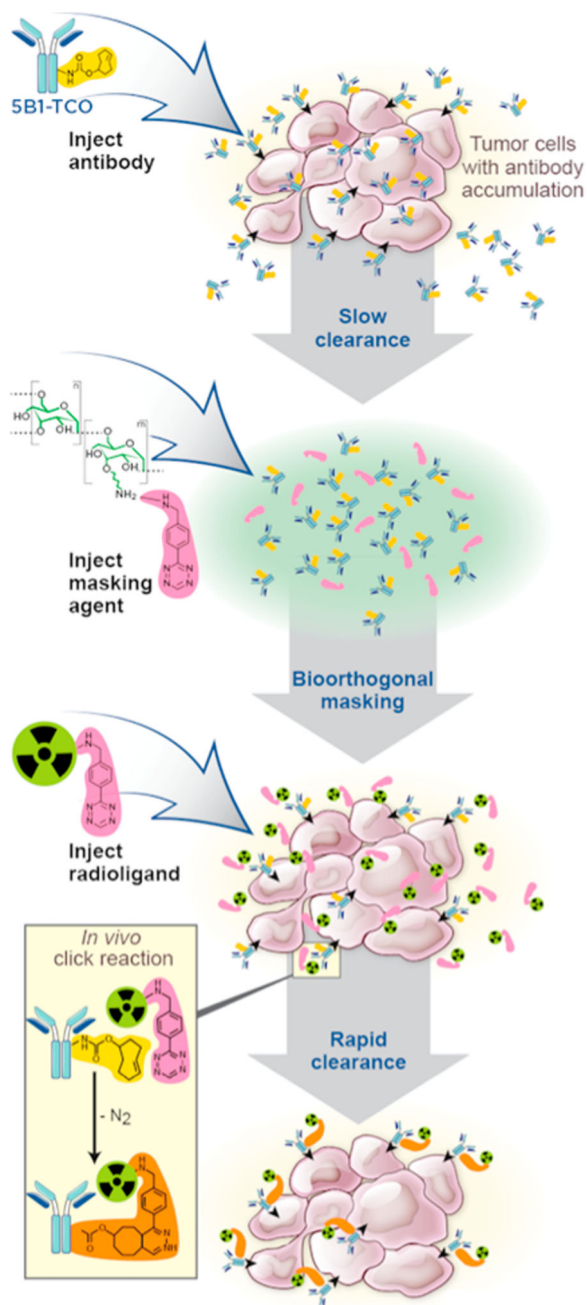
## ABBREVIATIONS

<b>PET</b>	positron emission tomography
<b>IEDDA</b>	inverse electron-demand Diels–Alder
<b>TTB</b>	tumor-to-blood
<b>Tz</b>	tetrazine
<b>TCO</b>	<i>trans</i> -cyclooctene
<b>DP</b>	dextran polymer

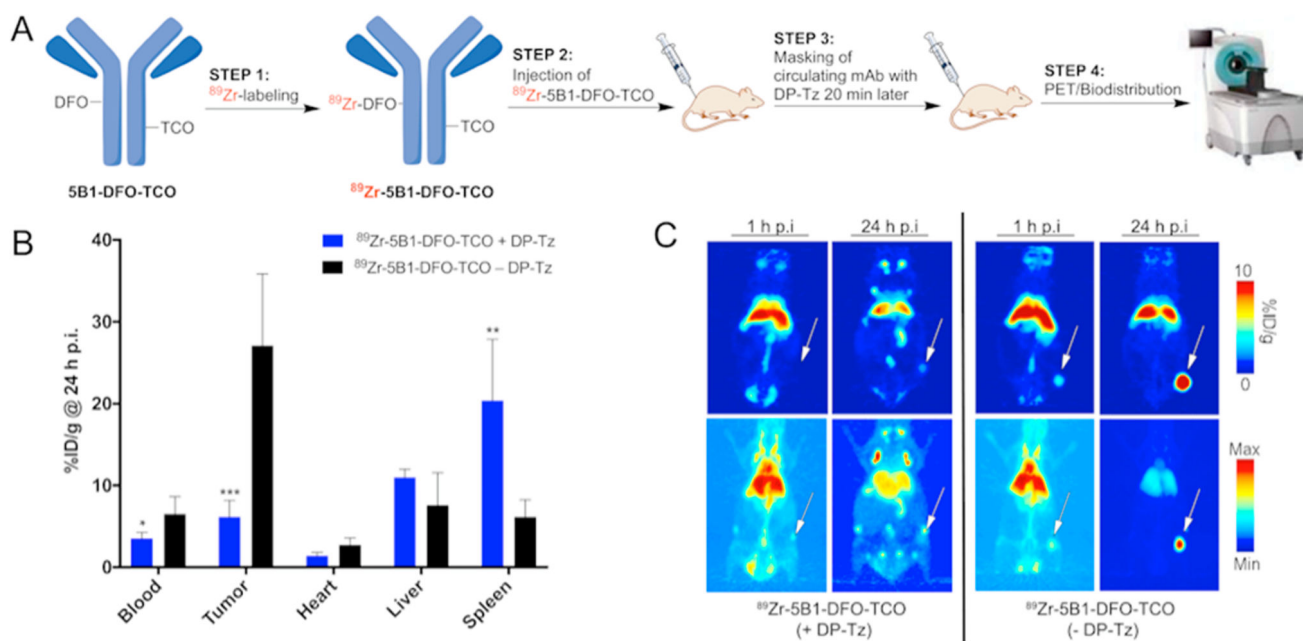
## References

1. Wilson R, Spiller DG, Beckett A, Prior IA, See V. Highly Stable Dextran-Coated Quantum Dots for Biomolecular Detection and Cellular Imaging. *Chem. Mater.* 2010; 22:6361–6369.
2. Mehvar R. Dextran for targeted and sustained delivery of therapeutic and imaging agents. *J. Controlled Release.* 2000; 69:1–25.
3. Sinha VR, Kumria R. Colonic drug delivery: prodrug approach. *Pharm. Res.* 2001; 18:557–564. [PubMed: 11465408]
4. Terg R, Miguez CD, Castro L, Araldi H, Dominguez S, Rubio M. Pharmacokinetics of Dextran-70 in patients with cirrhosis and ascites undergoing therapeutic paracentesis. *J. Hepatol.* 1996; 25:329–333. [PubMed: 8895012]
5. Behe M, Du J, Becker W, Behr T, Angerstein C, Marquez M, Hiltunen J, Nilsson S, Holmberg AR. Biodistribution, blood half-life, and receptor binding of a somatostatin-dextran conjugate. *Med. Oncol.* 2001; 18:59–64. [PubMed: 11778971]
6. Dreher MR, Liu W, Michelich CR, Dewhirst MW, Yuan F, Chilkoti A. Tumor vascular permeability, accumulation, and penetration of macromolecular drug carriers. *J. Natl. Cancer Inst.* 2006; 98:335–344. [PubMed: 16507830]
7. Houghton JL, Membreno R, Abdel-Atti D, Cunanan KM, Carlin S, Scholz WW, Zanzonico PB, Lewis JS, Zeglis BM. Establishment of the In Vivo Efficacy of Pretargeted Radioimmunotherapy Utilizing Inverse Electron Demand Diels-Alder Click Chemistry. *Mol. Cancer Ther.* 2017; 16:124–133. [PubMed: 28062708]
8. Meyer JP, Houghton JL, Kozlowski P, Abdel-Atti D, Reiner T, Pillarsetty NV, Scholz WW, Zeglis BM, Lewis JS. 18)F-Based Pretargeted PET Imaging Based on Bioorthogonal Diels-Alder Click Chemistry. *Bioconjugate Chem.* 2016; 27:298–301.
9. Zeglis BM, Sevak KK, Reiner T, Mohindra P, Carlin SD, Zanzonico P, Weissleder R, Lewis JS. A pretargeted PET imaging strategy based on bioorthogonal Diels-Alder click chemistry. *J. Nucl. Med.* 2013; 54:1389–1396. [PubMed: 23708196]

10. Rossin R, Verkerk PR, van den Bosch SM, Vulderson RC, Verel I, Lub J, Robillard MS. In vivo chemistry for pretargeted tumor imaging in live mice. *Angew. Chem., Int. Ed.* 2010; 49:3375–3378.
11. Houghton JL, Zeglis BM, Abdel-Atti D, Sawada R, Scholz WW, Lewis JS. Pretargeted Immuno-PET of Pancreatic Cancer: Overcoming Circulating Antigen and Internalized Antibody to Reduce Radiation Doses. *J. Nucl. Med.* 2016; 57:453–459. [PubMed: 26471693]
12. Blackman ML, Royzen M, Fox JM. Tetrazine ligation: fast bioconjugation based on inverse-electron-demand Diels-Alder reactivity. *J. Am. Chem. Soc.* 2008; 130:13518–13519. [PubMed: 18798613]
13. Zeglis BM, Brand C, Abdel-Atti D, Carnazza KE, Cook BE, Carlin S, Reiner T, Lewis JS. Optimization of a Pretargeted Strategy for the PET Imaging of Colorectal Carcinoma via the Modulation of Radioligand Pharmacokinetics. *Mol. Pharmaceutics.* 2015; 12:3575–3587.
14. Houghton JL, Zeglis BM, Abdel-Atti D, Aggeler R, Sawada R, Agnew BJ, Scholz WW, Lewis JS. Site-specifically labeled CA19.9-targeted immunoconjugates for the PET, NIRF, and multimodal PET/NIRF imaging of pancreatic cancer. *Proc. Natl. Acad. Sci. U. S. A.* 2015; 112:15850–15855. [PubMed: 26668398]
15. Lappchen T, Rossin R, van Mourik TR, Gruntz G, Hoeben FJM, Versteegen RM, Janssen HM, Lub J, Robillard MS. DOTA-tetrazine probes with modified linkers for tumor pretargeting. *Nucl. Med. Biol.* 2017; 55:19–26. [PubMed: 29028502]
16. Meyer JP, Kozlowski P, Jackson J, Cunanan KM, Adumeau P, Dilling TR, Zeglis BM, Lewis JS. Exploring Structural Parameters for Pretargeting Radioligand Optimization. *J. Med. Chem.* 2017; 60:8201–8217. [PubMed: 28857566]
17. Altai M, Membreno R, Cook B, Tolmachev V, Zeglis BM. Pretargeted Imaging and Therapy. *J. Nucl. Med.* 2017; 58:1553–1559. [PubMed: 28687600]
18. Cheal SM, Xu H, Guo HF, Lee SG, Punzalan B, Chalasani S, Fung EK, Jungbluth A, Zanzonico PB, Carrasquillo JA, et al. Theranostic pretargeted radioimmunotherapy of colorectal cancer xenografts in mice using picomolar affinity (8)(6)Y-or (1)(7)(7)Lu-DOTA-Bn binding scFv C825/GPA33 IgG bispecific immunoconjugates. *Eur. J. Nucl. Med. Mol. Imaging.* 2016; 43:925–937. [PubMed: 26596724]
19. Cheal SM, Xu H, Guo HF, Zanzonico PB, Larson SM, Cheung NK. Preclinical evaluation of multistep targeting of diasialoganglioside GD2 using an IgG-scFv bispecific antibody with high affinity for GD2 and DOTA metal complex. *Mol. Cancer Ther.* 2014; 13:1803–1812. [PubMed: 24944121]
20. Rossin R, Lappchen T, van den Bosch SM, Laforest R, Robillard MS. Diels-Alder reaction for tumor pretargeting: in vivo chemistry can boost tumor radiation dose compared with directly labeled antibody. *J. Nucl. Med.* 2013; 54:1989–1995. [PubMed: 24092936]
21. Orcutt KD, Rhoden JJ, Ruiz-Yi B, Frangioni JV, Wittrup KD. Effect of small-molecule-binding affinity on tumor uptake in vivo: a systematic study using a pretargeted bispecific antibody. *Mol. Cancer Ther.* 2012; 11:1365–1372. [PubMed: 22491799]
22. Green DJ, Frayo SL, Lin Y, Hamlin DK, Fisher DR, Frost SH, Kenoyer AL, Hylarides MD, Gopal AK, Gooley TA, et al. Comparative Analysis of Bispecific Antibody and Streptavidin-Targeted Radioimmunotherapy for B-cell Cancers. *Cancer Res.* 2016; 76:6669–6679. [PubMed: 27590740]
23. Devaraj NK, Thurber GM, Keliher EJ, Marinelli B, Weissleder R. Reactive polymer enables efficient in vivo bioorthogonal chemistry. *Proc. Natl. Acad. Sci. U. S. A.* 2012; 109:4762–4767. [PubMed: 22411831]
24. Seitchik JL, Peeler JC, Taylor MT, Blackman ML, Rhoads TW, Cooley RB, Refakis C, Fox JM, Mehl RA. Genetically encoded tetrazine amino acid directs rapid site-specific in vivo bioorthogonal ligation with trans-cyclooctenes. *J. Am. Chem. Soc.* 2012; 134:2898–2901. [PubMed: 22283158]
25. Nishikawa M, Yamashita F, Takakura Y, Hashida M, Sezaki H. Demonstration of the receptor-mediated hepatic uptake of dextran in mice. *J. Pharm. Pharmacol.* 1992; 44:396–401. [PubMed: 1279155]

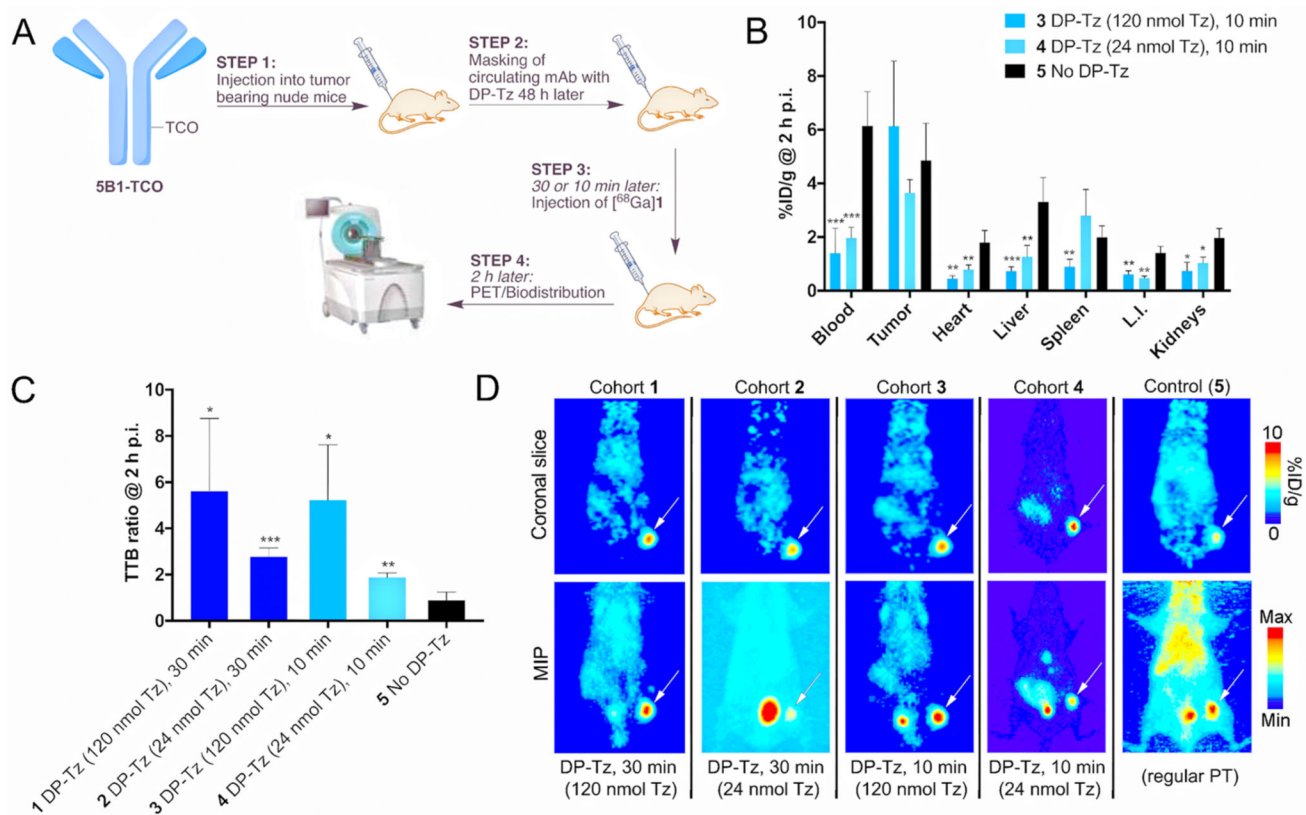


**Figure 1.** Schematic of the modified IEDDA-based pretargeting approach including the injection of the masking agent prior to the radioligand.

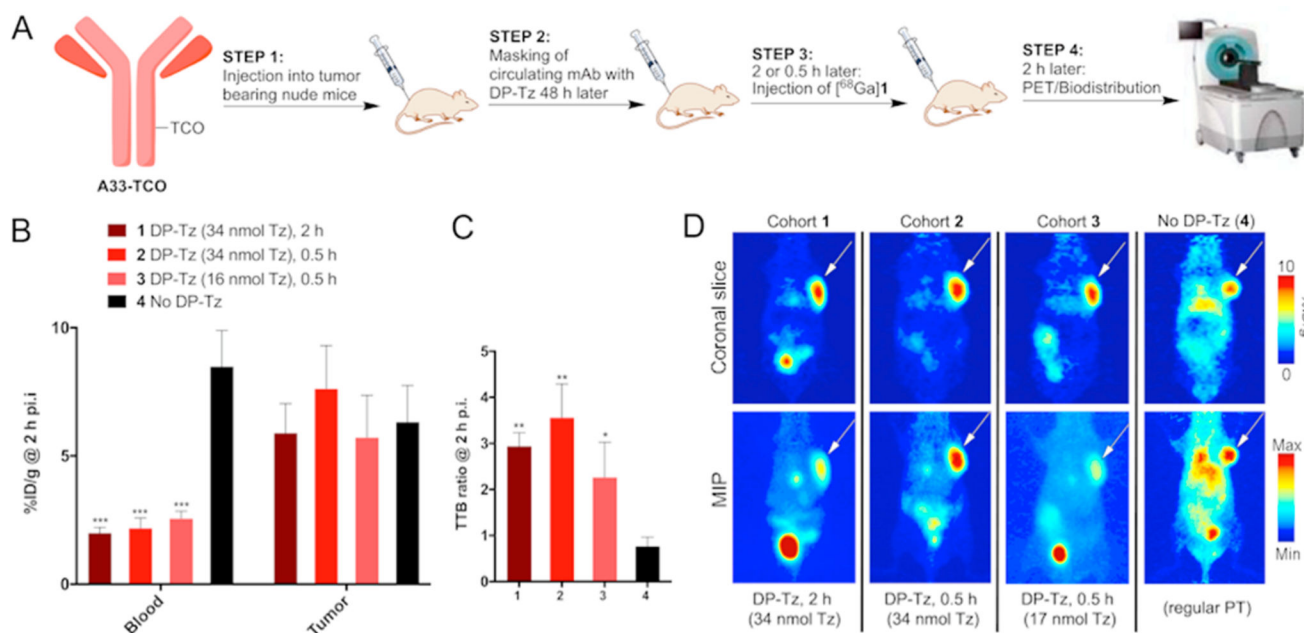


**Figure 2.**

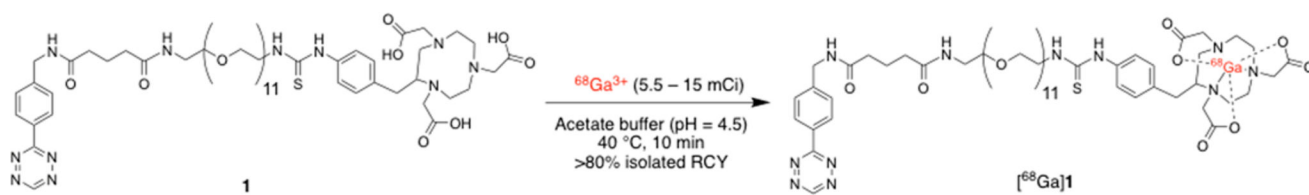
(A) Experimental scheme. (B) Ex *in vivo* biodistribution data ( $n = 5$ ) of  $^{89}\text{Zr}$ -labeled 5B1–TCO–DFO alone or after injection (20 min after 5B1) of DP–Tz at the 24 h time point (post mAb injection). (C) Complementary PET imaging data showing the biodistribution of  $^{89}\text{Zr}$ -labeled 5B1–TCO–DFO with (left side) and without (right side) DP–Tz 1 and 24 h post mAb injection.

**Figure 3.**

(A) Experimental scheme. (B) Full pretargeted *ex vivo* biodistribution of BxPC3-tumor bearing mice that were injected 10 min prior to the radioligand with either high (120 nmol Tz) or low (24 nmol Tz) amounts of DP-Tz. (C) *Ex vivo* tumor-to-blood (TTB) ratios obtained for different amounts of DP-Tz and lag times between DP-Tz and radiotracer injection. (D) Corresponding PET images showing the significantly improved TTB ratios using the newly developed DP-Tz.

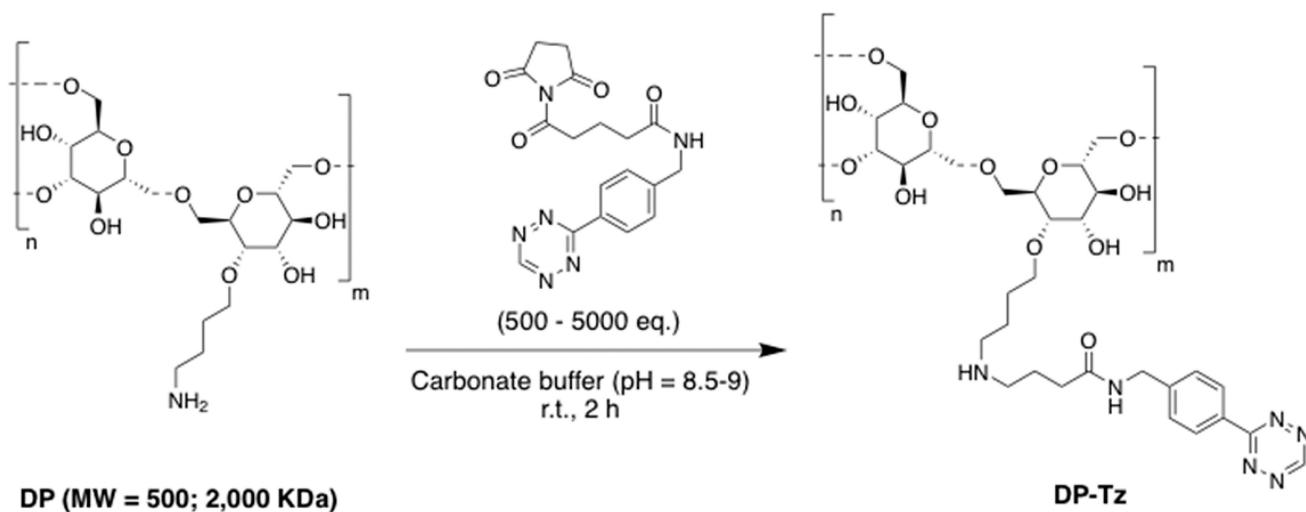


**Figure 4.** *Ex vivo* biodistribution and PET imaging data obtained 2 h post injection of  $[^{68}\text{Ga}]\mathbf{1}$ . (A) Experimental scheme. (B) Absolute blood and tumor radioactivity concentrations 2 h post injection. (C) *Ex vivo* tumor-to-blood (TTB) ratios calculated for different amounts of DP-Tz and lag times between DP-Tz and radiotracer injection. (D) Corresponding PET images showing the significant improvements in TTB ratios achieved with the newly developed DP-Tz.



**Scheme 1.**  
Radiolabeling of NOTA-PEG<sub>11</sub>-Tz Precursor 1 with  $^{68}\text{Ga}$  To Yield the Tetrazine Radioligand  $[^{68}\text{Ga}]\text{Ga-NotA-PEG}_{11}\text{-Tz}$  ( $[^{68}\text{Ga}]1$ )



**Scheme 2.**

Amine-Functionalized Dextran Polymers (DP-NH<sub>2</sub>) Were Incubated with Tz-NHS Ester To Form Tetrazine-Modified Dextran Polymers (DP-Tz)<sup>a</sup>

<sup>a</sup>DP-Tz was obtained in high isolated yields (>75%), with Tz/DP ratios of 62–654, depending on DP-NH<sub>2</sub> starting material and reaction conditions (Table S1).